

AFM-based dual nano-mechanical phenotypes for cancer metastasis

Soyeun Park · Yong J. Lee

Received: 3 February 2014 / Accepted: 5 May 2014 / Published online: 30 June 2014
© Springer Science+Business Media Dordrecht 2014

Abstract An enhanced mechanical compliance is considered to be a mechanical indicator for metastatic cancer cells. Our study using atomic force microscopy (AFM) revealed that breast cancer cells agreed well with this hypothesis. However, prostate cancer cells displayed a reverse correlation; less metastatic prostate cancer cells were more mechanically compliant. Two-dimensional AFM force spectroscopy was performed to characterize dual mechanical properties—the cell–substrate adhesion as well as the mechanical compliance. Interestingly, prostate cancer cells displayed a strong positive correlation between the cell–substrate adhesion and metastatic potential. However, there was no clearly observable correlation between the cell–substrate adhesion and the metastatic potential despite variations in mechanical compliance of breast cancer cells. These results suggest that the correlation between the dual mechanical signatures and metastatic potential be uniquely identified for cancer cells originating from different organs. We postulate that this correlation could reveal which step of cancer progression is favorable in terms of physical interaction between cancer cells and micro-environments. We expect that based on the “seed and soil hypothesis”, the identification of the dual mechanical phenotypes, could provide a new insight for understanding how a dominant metastatic site is determined for cancer cells originating from specific organs.

Keywords Atomic force microscopy · Force spectroscopy · Metastatic potential · Mechano-phenotype · Cell–substrate adhesion · Mechanical compliance

Metastasis is a major cause for cancer-related mortality. In addition to epigenic factors and biochemical interaction, the physical interaction of cancer cells with microenvironments has recently been noticed to contribute to cancer progression [1]. During the complex metastatic process, cancer cells are doomed to negotiate their mechanical properties including mechanical compliance, motility, cell–cell adhesion, and cell–substrate adhesions [2–5]. Over the past decade, many studies have investigated whether an enhanced mechanical compliance, which is expected to be beneficial for extra/intravasation and invasion, can be utilized as a

S. Park (✉)
College of Pharmacy, Keimyung University, Daegu, South Korea
e-mail: sypark20@kmu.ac.kr

Y. J. Lee
School of Mechanical Engineering, Kyungpook National University, Daegu, South Korea

universal marker for cancer metastasis [6, 7]. Against this optimistic prediction, recent studies reported an unequivocal correlation between mechanical compliance and metastatic progression [8–10]. These findings suggest that it is important to carefully investigate the key mechanical properties at each step of metastatic progression [11]. Nevertheless, the lack of emerging techniques to elucidate the complex nature of metastasis hinders a clear investigation of multifaceted contribution of mechanical phenotypes of cancer cells to cancer progression.

In this study, AFM force spectroscopy was utilized to characterize cell–substrate adhesion as well as the mechanical compliance of cancer cells with distinct metastatic potentials. As a model, we used highly (CL-1) and lowly (LNCaP) metastatic prostate and highly (MD-MB-231) and lowly (MCF-7) metastatic breast cancer cell lines [12, 13]. The cells were grown on pre-sterilized glass slides (Erie Scientific, Portsmouth, NH, USA) 1 day before the AFM data were taken.

All AFM measurements were taken with an MFP 3D (Asylum Research, Santa Barbara, CA, USA) mounted on an inverted optical microscope (IX-81, Olympus, Tokyo, Japan). The physiological temperature and a liquid environment were maintained by a fluid cell and Bioheater. V-shaped silicon nitride cantilevers (typical spring constant ~ 0.01 N/m) modified with polystyrene beads (typically $4.5 \mu\text{m}$) were used in order to obtain a well-defined contact area and to reduce the stress from otherwise sharp AFM tips. In order to obtain the elastic moduli, the force–distance (f – d) curves were acquired with a 1-s time interval, i.e., 1 Hz, with the trigger force of 100 pN at cell centers (Fig. 1a). The 2D array of f – d curves were obtained from a single cell or a part of a single cell with the trigger force of 100 pN and the indentation speed of 1.5–2.3 nm/s. Five to ten independent experiments were repeated for each cell line.

In order to determine the elastic moduli, the obtained f – d curves were converted to the force–indentation (f – δ) curves. The Hertz model was applied to determine the elastic moduli from f – δ curves. According to the analytical expression of the Hertz model,

$$K = \frac{E}{(1-\nu^2)} = \frac{3}{4} \frac{f}{\sqrt{R\delta^3}} \quad (1)$$

the f – δ curve can be converted to the curve of elastic constant $K=E/(1-\nu^2)$ versus the dimensionless quantity δ/R , where the R is the radius of the spherical tip and ν is the Poisson ratio. In the regions where the Hertz model fails to correctly deduce elastic constants due to strong substrate effects, advanced models, the Tu and the Chen models, were adopted. The local variations of the cell-adhesion properties were identified from the boundary conditions of the models best describing the elastic behavior from the f – δ curves. Whereas the Chen model considers a cell as a well-adhered layer on a hard substrate, the Tu model does it as a freely sliding layer. The details of experimental procedures are described elsewhere [11, 14].

In order to compare the mechanical compliance of all the investigated cell lines, the average elastic moduli at the cell centers were determined by the Hertz model. Typical f – δ curves obtained from the cell centers of breast and prostate cancer cells are shown in Fig. 1a. We found that the average elastic moduli of MD-MB231 were significantly lower than those of MCF-7 (Fig. 1b). This agrees well with the general expectation that enhanced mechanical compliance is suggested for highly metastatic cells involving a substantial mechanical deformation [15]. However, for prostate cancer cells, the dependence of mechanical compliance on metastatic potential was reversed. We found that CL-1 cells were mechanically stiffer than LNCaP cells (Fig. 1b). This nano-mechanical result agrees well with previous AFM studies on prostate cancer cells [8, 11]. These unequivocal correlations from the breast and prostate cancer cells imply that the mechanical compliance assay alone cannot sufficiently represent the mechano-

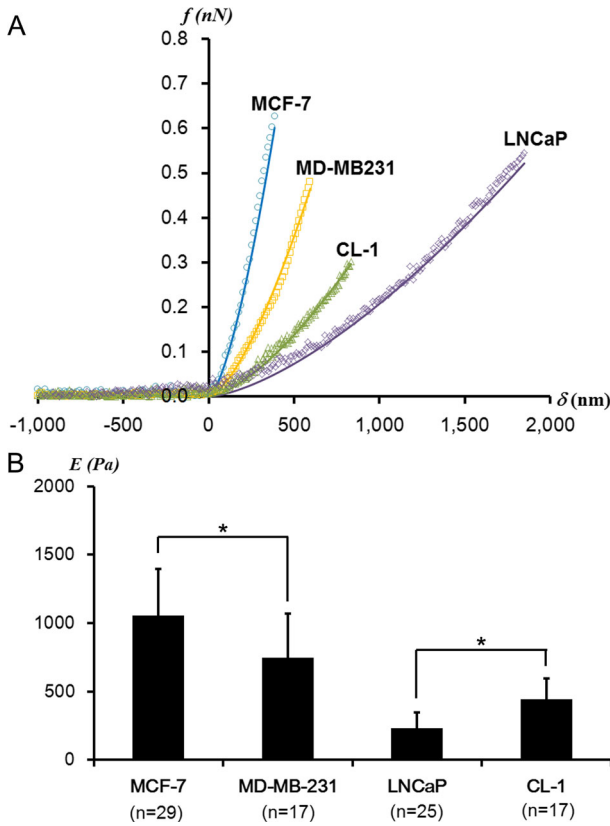


Fig. 1 **a** Representative f - δ curves obtained from prostate—CL-1 and LNCaP—and breast—MCF-7 and MD-MB231—cancer cells. The data obtained from the cell centers (*dots*) fit well with the Hertz model (solid lines). **(b)** The average elastic moduli determined from CL-1, LNCaP, MCF-7, and MD-MB231 cells at cell centers ($*p < 0.01$). n indicates the number of cells investigated. There is no statistical difference in the trigger forces applied on all investigated cells

phenotype characteristic for cancer metastasis. More information is required in order to corroborate the correlation between the mechanical phenotype and cancer metastasis for specific organs.

Cancer cells undergo a unique mechano-reciprocity with the microenvironment at each step of the metastatic progression [16]. Followed by the primary tumor proliferation and angiogenesis, the metastatic cascade begins with a detachment of cancer cells from the epithelium. The subsequent invasion, intra/extravasation and the formation of a secondary tumor involve significant cell–cell and cell–substrate adhesions under the influence of diverse microenvironments [1, 5]. A dynamic modulation of cellular adhesion might occur during each progression step [3]. In this study, we determined the cell–substrate adhesion properties by utilizing AFM force spectroscopy. As described earlier, by utilizing the mathematical models considering the different boundary conditions, the cell–substrate adhesion was determined for a local nano-domain of a cell. As shown in Fig. 2a–b, the CL-1 cells were primarily analyzed by the Chen model assuming the well-adhered layers on the substrate, while the Hertz model was mostly used to analyze the LNCaP cells. However, we did not observe any difference in the local variation of the models between MCF-7 and MD-MB231 cells (Fig. 2c–d).

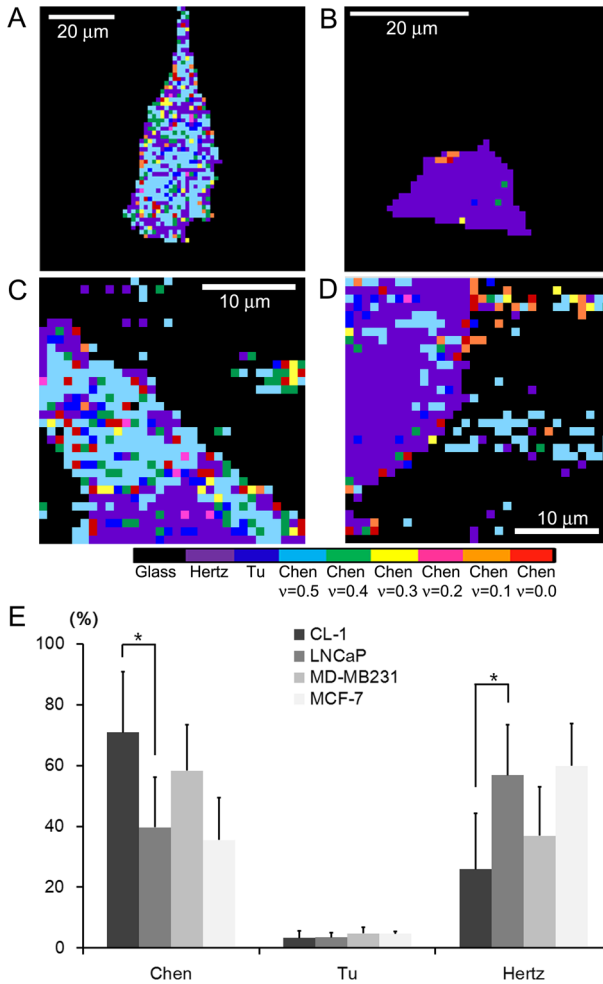


Fig. 2 Adhesion maps derived from 2D f - d curves obtained from **a** CL-1, **b** LNCaP, **c** MD-MB231, and **d** MCF-7 cells. The resolutions of images are 1.27 μm , 1.00 μm , 1.56 μm , and 0.97 μm per pixel for **(a)**, **(b)**, **(c)**, and **(d)**, respectively. The adhesion maps were acquired by determining the mathematical model that best describes the homogeneous elastic behavior for local nano-domains of a cell. The colors correspond to the following models except for black representing the glass substrates: from left to right, the Hertz, the Tu, and the Chen models with varying Poisson ratio of 0.5, 0.4, 0.3, 0.2, 0.1, and 0.0. The Chen model represents well-adhered regions of cells on a substrate. **e** The mathematical model yielding the most constant elastic moduli over the observed indentation range was counted for each cell line. Compared to LNCaP cells, the Chen model was primarily adopted to calculate the elastic moduli of CL-1 cells, indicating an enhancement of the cell-substrate adhesion ($*p < 0.01$). We did not observe any significant difference in the mathematical models used between breast cancer cells. The Tu model was hardly used for the cells investigated

Note that breast cancer cells were investigated over a limited part of a cell region due to their thickness variations outside the vertical range of the AFM scanner (15 μm). The entire region of the prostate cancer cells was investigated by AFM. As shown in Fig. 2e, we counted the number of the mathematical models best describing the elastic behavior of nano-domains of investigated cells. The Chen model was highly utilized to analyze the f - δ curves obtained from the CL-1 cells. The adoption occurrence of the Chen model is much

higher for CL-1 cells than for LNCaP cells ($p < 0.01$). This result implies that the cell–substrate adhesion displays a strong correlation with metastatic potential for the prostate cancer cells. The adoption frequency of the Chen model is comparable for both breast cancer cell lines, indicating that the adhesion properties of the breast cancer cell lines are similar. The focal adhesion representing the cell–substrate adhesion is known to nucleate the actin microfilaments governing the cellular structural integrity and mechanical stiffness. An enhanced adhesion observed in CL-1 cells consistently supports the increase in mechanical stiffness, i.e., elastic moduli compared to LNCaP cells. As for breast cancer cells, the observed similarity in cell–substrate adhesion implies no significant difference in the nucleation of actin microfilaments. A decrease in the elastic moduli observed from MD-MB231 cells might originate from either the constitutional difference of the actin cytoskeleton or other cellular organelles. Recently, the keratin intermediate filaments were noticed as a major contributor to cellular mechanical resilience [17].

From AFM results, we found that prostate and breast cancer cells display an inconsistency in the mechano-phenotypes representing a high metastatic potential. Highly metastatic prostate cancer cells show a decrease in the mechanical compliance and an increase in the cell–substrate adhesion. However, an enhanced mechanical compliance with a similar cell–substrate adhesion is identified as a typical mechano-phenotype of highly metastatic breast cancer cells. Despite no difference in the blood flow, the “seed and soil” hypothesis states that a tumor cell metastasizes to a specific organ just as a seed grows well on a land with fertile soil [18]. Prostate cancer cells are known to metastasize well to bones, whereas breast cancer cells metastasize dominantly to the liver and lungs [19, 20]. We can conjecture that metastasis seems to be successful only when cancer cells acquire the necessary traits to overcome the physical barriers as well as other environmental conditions. Several studies revealed that metastasis of breast cancer cells to the lung and liver is mainly mediated by an abnormally enhanced adhesion to the vasculature via specific proteins such as selectin and integrin [21, 22]. This molecular insight supports our AFM-based adhesion assay. In Fig. 2e, comparing with the Chen model, the Tu model, considering a freely sliding layer on a substrate, is rarely optimal for the breast cancer cells investigated. This result indicates strong cell–substrate adhesions of breast cancer cells. However, the difference in the cell–substrate adhesion is hardly noticed between MCF-7 and MD-MB231 cells, while a significant difference in the mechanical compliance exists between them. The initial arrest of the breast cancer cells in the capillary beds is thought to contribute to metastasis. However, our results imply that the physical break-through in the vascular endothelium or the basement of the host cells, which can be benefited by the enhanced mechanical compliance, needs to be considered as a more critical step. On the other hand, our mechanical compliance assay reveals that the mechanical compliance is impaired in highly metastatic prostate cancer cells (Fig. 1b). In terms of the physical interaction of cancer cells with microenvironments, our data suggests that despite the physical difficulties in invasion due to impaired mechanical compliance, metastasis of prostate cancer cells can be facilitated by a significantly enhanced cell–substrate adhesion. It is being increasingly recognized that prostate cancer cell interactions with a bone microenvironment initiate a complex and vicious cycle accompanying regulatory factors such as matrix metalloproteinases [23]. Together with our AFM results, we postulate that it is relatively easy to overcome a deficiency in mechanical compliance of prostate cancer cells by several regulatory factors in a bone microenvironment. However, the initial arrest of prostate cancer cells facilitated by enhanced cell–substrate adhesion might be a critical step for cancer progression. Our study using prostate and breast cancer cells suggests that a differentiated diagnostic and therapeutic strategy be applied to each type of cancer in order to protect the patients from metastasis.

We conclude that mechanical compliance alone fails to serve as a universal indicator for metastatic progression, but AFM-based characterization of mechano-phenotype utilizing the dual mechanical properties of mechanical compliance and cell-substrate adhesion might provide dual mechanical properties (mechanical compliance and cell-substrate adhesion) might provide critical phenomenological information for a critical step of metastasis for different types of cancer. Although more precise molecular mechanisms correlating the phenomenological information remains to be elucidated, we believe that our AFM-based dual mechano-phenotype provides a novel approach which ultimately may be applicable for the identification of therapeutic targets and for the enhancement of drug efficacy for advanced cancer patients.

Acknowledgments This research was supported by College of Pharmacy-specialized Research Fund (from the Institute for New Drug Development) of Keimyung University in 2012.

Conflict of interest The authors declare that there are no conflicts of interest related to this work.

References

1. Wirtz, D., Konstantopoulos, K., Searson, P.C.: The physics of cancer: the role of physical interactions and mechanical forces in metastasis. *Nat. Rev. Cancer* **11**(7), 512–522 (2011)
2. Suresh, S.: Biomechanics and biophysics of cancer cells. *Acta Mater.* **55**(12), 3989–4014 (2007)
3. Hehlhans, S., Haase, M., Cordes, N.: Signalling via integrins: implications for cell survival and anticancer strategies. *Biochim. Biophys. Acta* **1775**(1), 163–180 (2007). doi:10.1016/j.bbcan.2006.09.001
4. Pillet, F., Chopinet, L., Formosa, C., Dague, E.: Atomic force microscopy and pharmacology: from microbiology to cancerology. *Biochim. Biophys. Acta* **1840**(3), 1028–1050 (2014). doi:10.1016/j.bbagen.2013.11.019
5. Kumar, S., Weaver, V.: Mechanics, malignancy, and metastasis: the force journey of a tumor cell. *Cancer Metastasis Rev.* **28**(1–2), 113–127 (2009)
6. Remmerbach, T.W., Wottawah, F., Dietrich, J., Lincoln, B., Wittekind, C., Guck, J.: Oral cancer diagnosis by mechanical phenotyping. *Cancer Res.* **69**(5), 1728–1732 (2009)
7. Ochalek, T., Nordt, F.J., Tullberg, K., Burger, M.M.: Correlation between cell deformability and metastatic potential in B16-F1 melanoma cell variants. *Cancer Res.* **48**(18), 5124–5128 (1988)
8. Faria, E.C., Ma, N., Gazi, E., Gardner, P., Brown, M., Clarke, N.W., Snooka, R.D.: Measurement of elastic properties of prostate cancer cells using AFM. *Analyst* **133**(11), 1498–1500 (2008)
9. Darling, E.M., Zauscher, S., Block, J.A., Guilak, F.: A thin-layer model for viscoelastic, stress-relaxation testing of cells using atomic force microscopy: do cell properties reflect metastatic potential? *Biophys. J.* **92**(5), 1784–1791 (2007)
10. Zhang, G., Long, M., Wu, Z.Z., Yu, W.Q.: Mechanical properties of hepatocellular carcinoma cells. *World J. Gastroenterol.* **8**(2), 243–246 (2002)
11. Bastatas, L., Martinez-Marin, D., Matthews, J., Hashem, J., Lee, Y.J., Sennoune, S., Filleur, S., Martinez-Zaguilan, R., Park, S.: AFM nano-mechanics and calcium dynamics of prostate cancer cells with distinct metastatic potential. *Biochim. Biophys. Acta* **1820**(7), 1111–1120 (2012). doi:10.1016/j.bbagen.2012.02.006
12. Horoszewicz, J.S., Leong, S.S., Kawinski, E., Karr, J.P., Rosenthal, H., Chu, T.M., Mirand, E.A., Murphy, G.P.: LNCaP model of human prostatic-carcinoma. *Cancer Res.* **43**(4), 1809–1818 (1983)
13. Hugué, E.L., McMahon, J.A., McMahon, A.P., Bicknell, R., Harris, A.L.: Differential expression of human Wnt gene-2, gene-3, gene-4, and gene-7b in human breast cell-lines and normal and disease states of human breast-tissue. *Cancer Res.* **54**(10), 2615–2621 (1994)
14. Mahaffy, R.E., Park, S., Gerde, E., Kas, J., Shih, C.K.: Quantitative analysis of the viscoelastic properties of thin regions of fibroblasts using atomic force microscopy. *Biophys. J.* **86**(3), 1777–1793 (2004)
15. Guck, J., Schinkinger, S., Lincoln, B., Wottawah, F., Ebert, S., Romeyke, M., Lenz, D., Erickson, H.M., Ananthakrishnan, R., Mitchell, D., Kas, J., Ulvick, S., Bilby, C.: Optical deformability as an inherent cell marker for testing malignant transformation and metastatic competence. *Biophys. J.* **88**(5), 3689–3698 (2005)
16. Hanahan, D., Weinberg, R.A.: Hallmarks of cancer: the next generation. *Cell* **144**(5), 646–674 (2011)

17. Seltmann, K., Fritsch, A.W., Kas, J.A., Magin, T.M.: Keratins significantly contribute to cell stiffness and impact invasive behavior. *Proc. Natl. Acad. Sci. U. S. A.* **110**(46), 18507–18512 (2013). doi:[10.1073/pnas.1310493110](https://doi.org/10.1073/pnas.1310493110)
18. Paget, S.: The distribution of secondary growths in cancer of the breast. *Lancet* **1**, 571–573 (1889)
19. Bubendorf, L., Schopfer, A., Wagner, U., Sauter, G., Moch, H., Willi, N., Gasser, T.C., Mihatsch, M.J.: Metastatic patterns of prostate cancer: an autopsy study of 1,589 patients. *Hum. Pathol.* **31**(5), 578–583 (2000)
20. Chambers, A.F., Groom, A.C., MacDonald, I.C.: Dissemination and growth of cancer cells in metastatic sites. *Nat. Rev. Cancer* **2**(8), 563–572 (2002). doi:[10.1038/nrc865](https://doi.org/10.1038/nrc865)
21. Wang, H., Fu, W., Im, J.H., Zhou, Z., Santoro, S.A., Iyer, V., DiPersio, C.M., Yu, Q.C., Quaranta, V., Al-Mehdi, A., Muschel, R.J.: Tumor cell alpha3beta1 integrin and vascular laminin-5 mediate pulmonary arrest and metastasis. *J. Cell Biol.* **164**(6), 935–941 (2004). doi:[10.1083/jcb.200309112](https://doi.org/10.1083/jcb.200309112)
22. Laubli, H., Stevenson, J.L., Varki, A., Varki, N.M., Borsig, L.: L-selectin facilitation of metastasis involves temporal induction of Fut7-dependent ligands at sites of tumor cell arrest. *Cancer Res.* **66**(3), 1536–1542 (2006). doi:[10.1158/0008-5472.can-05-3121](https://doi.org/10.1158/0008-5472.can-05-3121)
23. Roudier, M.P., Corey, E., True, L.D., Hiagno, C.S., Ott, S.M., Vessell, R.L.: Histological, immunophenotypic and histomorphometric characterization of prostate cancer bone metastases. *Cancer Treat. Res.* **118**, 311–339 (2004)